Biomethanation of syngas by enriched mixed anaerobic consortium in pressurized agitated column

J. Figueras, H. Benbelkacem, C. Dumas, Pierre Buffière

Journal Pre-proofs

"Biomethanation of Syngas by Enriched Mixed Anaerobic Consortium in Pressurized agitated column"

J. Figueras, H. Benbelkacem, C. Dumas, P. Buffiere

PII: S0960-8524(21)00889-0
DOI: https://doi.org/10.1016/j.biortech.2021.125548
Reference: BITE 125548

To appear in: *Bioresource Technology*

Received Date: 21 May 2021
Revised Date: 6 July 2021
Accepted Date: 9 July 2021

Please cite this article as: Figueras, J., Benbelkacem, H., Dumas, C., Buffiere, P., "Biomethanation of Syngas by Enriched Mixed Anaerobic Consortium in Pressurized agitated column", *Bioresource Technology* (2021), doi: https://doi.org/10.1016/j.biortech.2021.125548

"Biomethanation of Syngas by Enriched Mixed Anaerobic Consortium in Pressurized agitated column"

J. Figueras[a], H. Benbelkacem[a], C. Dumas[b], and P. Buffiere[a*]

[a]Univ Lyon, INSA Lyon, DEEP, EA7429, 69621 Villeurbanne, France
[b]TBI, University of Toulouse, INSA, INRAE, CNRS,Toulouse, France
*Corresponding author: Pierre Buffiere; Tel.: +334 72 4384-78; E-mail: pierre.buffiere@insa-lyon.fr

Abstract

In a circular economy approach, heterogeneous wastes can be upgraded to energy in the form of syngas via pyrogasification, and then to methane via biomethanation. Working at high pressure is a promising approach to intensify the process and to reduce gas-liquid transfer limitations. However, raising the pressure could lead to reaching the CO inhibition threshold of the microorganisms involved in syngas-biomethanation. To investigate the impact on pressure on the process, a 10L continuous stirred tank reactor working at 4 bars and 55°C was implemented. Syngas (40% CO, 40% H_2, 20% CO_2) biomethanation was performed successfully and methane productivity as high as 6.8 $mmol_{CH4}/L_{reactor}/h$ with almost full conversion of CO (97%) and H_2 (98%) was achieved. CO inhibition was investigated and carboxydotrophs appeared less resistant to high CO exposition than methanogens.

Keywords: Biomethanation, syngas, fermentation, carbon monoxide conversion, biological water-gas shift

1 Introduction

As the world population grows, waste management becomes an increasing issue. More and more heterogenous wastes including plastic are produced each year which leads to issues regarding health or environment. Waste management can then come at high cost for industries or public actors. In a circular economy perspective, gasification can help reducing overall waste and convert it to energy in the form of syngas, a mixture of N_2, H_2, CO, CO_2, and other minor compounds. Promising studies show that heterogenous wastes including plastics can be converted to syngas with gasification (Arena, 2012; Perkins, 2020). However, syngas has a relatively low calorific value. Its conversion into methane would then represent an interesting upgrade, considering the natural gas grid extent and storage infrastructure already in place in Europe. Moreover, syngas methanation features in the study "A 100% renewable gas mix in 2050?" conducted by ADEME (French Agency for Ecological Transition), which explores the conditions of the technical and economic feasibility of a gas system in 2050 based on 100% renewable gas in France. Thus, syngas methanation is a promising technology at the center of renewable energy transition plans.

$$CO + 3H_2 \rightarrow CH_4 + H_2O \quad (1)$$

$$4CO + 2H_2O \rightarrow CH_4 + 3CO_2 \quad (2)$$

$$4H_2 + CO_2 \rightarrow CH_4 + 2H_2O \quad (3)$$

Syngas conversion to methane can be performed via catalytic methanation (Eq. (1)) or biological methanation (Eq. (2) and (3)). Catalytic methanation of CO and CO_2 is a more mature process, however its higher sensitivity to impurities, especially H_2S and tar, might make it less relevant regarding syngas methanation. Biological methanation could be more

resilient to impurities in the feed gas and can be achieved under mild operating conditions. Indeed, it can be operated at ambient pressure and temperatures around 35-75°C, whereas catalytic methanation requires higher pressure and temperatures above 250°C (Grimalt-Alemany et al., 2018). Moreover, biomethanation can convert CO and H_2 independently, as different biological routes are involved as discussed below. This allows biomethanation to convert syngas independently from the CO/H_2 ratio.

Syngas biological methanation is generally performed by the syntrophic association of anaerobic microorganisms, whether using an association of pure cultures or an adapted mixed consortium. The consortium uses syngas as both carbon and energy source to support their growth and synthetize methane and carbon dioxide. Complex biochemical reactions are involved, carried out by different microbial groups. They can be identified using specific inhibitors such as bromoethane sulfonate (BES) for methanogens and vancomycin for bacteria (Oremland and Capone, 1988), implementing specific activity tests with CO, H_2/CO_2 or acetate as sole substrates and characterizing the microbial population. Regarding syngas-biomethanation, the main observed reactions are carboxydotrophic hydrogenogenesis (water-gas shift reaction), carboxydotrophic acetogenesis, homoacetogenesis, hydrogenotrophic methanogenesis and acetoclastic methanogenesis (Grimalt-Alemany et al., 2019) as described in **Fig. 1**. In addition, Li et al. (2020) have suggested that syntrophic acetate oxidation (SAO) could also occur in syngas-biomethanation processes. Direct CO methanogenesis (Eq.(2)) could theoretically be another conversion route, as Sipma et al. (2004) have suggested its occurrence in CO-biomethanation experiments. However, to our knowledge, it has not been observed in a syngas-biomethanation process to date.

The biological mechanisms involved in syngas conversion by a mixed microbial consortium strongly depend on the operating temperature. Grimalt-Alemany et al. (2019) have adapted the same inoculum to mesophilic or thermophilic conditions. Based on activity tests and microbial consortia analysis, they suggested that in mesophilic conditions, acetate seemed to be the main intermediate for CO conversion paired with H_2/CO_2 as second intermediates through water-gas shift. In addition, homoacetogens appeared to be active and in competition with methanogens for H_2/CO_2. This makes sense with regards to the kinetic parameters of the populations involved: known hydrogenotrophic methanogens have smaller μ_{max} in mesophilic conditions (0.02–2.6 day^{-1}) compared to homoacetogens (1.20–4.68 day^{-1}) (Rafrafi et al., 2020). On the other hand, in thermophilic conditions, Grimalt-Alemany et al. (2019) suggested that H_2/CO_2 seemed to be the main intermediate through water-gas shift reaction, with no acetogenic nor acetotrophic activity detected. These results are in accordance with other findings from CO-biomethanation studies, with acetate being the main intermediate for CO conversion in mesophilic conditions and H_2/CO_2 in thermophilic conditions (Guiot et al., 2011; Sipma et al., 2003).

In addition, the operating temperature also has an impact on the methane productivity, which was found to be generally more than twice higher in thermophilic conditions compared to mesophilic conditions (Asimakopoulos et al., 2020; Grimalt-Alemany et al., 2019; Youngsukkasem et al., 2015). Bu et al. (2018) also observed that higher CO and H_2 conversion efficiencies were achieved in thermophilic conditions (97.2% and 100% for CO and H_2, respectively) compared to extreme-thermophilic conditions (83.7% and 96.2% for CO and H_2, respectively). This indicates that thermophilic conditions could be more promising regarding the economic viability of the process.

Biomethanation of CO as sole substrate has been studied both in batch (Alves et al., 2013; Arantes et al., 2018; Sancho Navarro et al., 2016; Sipma et al., 2003) and continuous mode (Guiot et al., 2011, 2010; Luo et al., 2013). As it gives important insight on CO conversion routes, one should note that when reviewing literature, CO-biomethanation should be distinguished from syngas-biomethanation, as different microorganisms seem to be involved. Indeed, Alves (2013) observed that the same sludge enriched with either CO or syngas would adapt differently and the microbial composition would be different, as well as the observed reaction products.

Moreover, the enrichment strategy could have an impact on the capacity of the inoculum to adapt to syngas-biomethanation. Grimalt-Alemany et al. (2019) hypothesized that, compared to other publications (Alves et al., 2013), their success into carrying an enrichment with a partial pressure of CO of 0.4 atm using successive batch transfers was due to starting right away at the final CO pressure instead of gradually increasing it. This makes sense, as the enrichment culture technique appears to specialized a consortium after the 2nd to 3rd transfer (Beck, 1971). This tends to indicate that the most efficient enrichment strategy would be to start at the target partial pressures.

Nevertheless, the main limiting step of biomethanation is the necessity to transfer the gaseous substrates to the biological catalyst which is in aqueous phase (Asimakopoulos et al., 2018; Klasson et al., 1991).

$$Rt_i = k_L a_i * (H_{i,cp} * P_i - C_{i,L}) \quad (4)$$

The mass transfer rate of a specific substrate Rt_i [mol/(m^3.s] can be described by Eq.(4). It is linked to the mass transfer coefficient $k_L a_i$ [1/s], which can be influenced by reactor type and operating parameters. It is also correlated to the concentration gradient $(H_{i,cp} * P_i - C_{i,L})$,

with $H_{i,\,cp}$ [mol/(L.bar)] being the Henry's law constant, P_i [bar] the partial pressure of the gas and $C_{i,\,L}$ [mol/L] its concentration in the liquid phase. It appears that increasing the partial pressure of the substrates by increasing the overall pressure of the process can lead to better transfer performances. Therefore, a higher pressurized process can lead to intensified methane production, which is a significant step towards an industrial application.

However, with an intensified pressurized process, another limiting step of syngas biomethanation could be CO inhibition. An increase in CO partial pressure and thus in CO transfer rate can lead to high soluble CO concentrations. These high soluble CO concentrations could be close to inhibition level for the different microbial groups involved into biomethanation reactions. CO inhibition has mainly been studied with CO-biomethanation experiments (Guiot et al., 2011; Sancho Navarro et al., 2016) and methane production has been achieved using CO-biomethanation with CO partial pressures as high as 1.8 bar (Sipma et al., 2003). However, considering syngas-biomethanation, the highest CO partial pressure tested with successful methane production has been 0.56 bar (Westman et al., 2016; Youngsukkasem et al., 2015). As specializing a mixed consortium to syngas or CO could lead to different microbial communities, the CO inhibition limits could vary with the different species present and thus be different for syngas-biomethanation compared to CO-biomethanation. Therefore, information on the capacity of syngas-biomethanation to operate at higher CO partial pressure without inhibition is lacking.

Therefore, the aim of the present study was to operate a continuous lab-scale pilot at high pressure in thermophilic conditions, using a mixed microbial consortium. A pressurized agitated column has been chosen for this study. The achieved methane productivity was

compared to previous studies of different continuous operated reactors. Since CO inhibition is a central matter of syngas-biomethanation, this study aimed to explore high CO exposition starting with initial partial pressure as high as 1.6 bar to investigate the resilience and adaptability of the consortium.

2 Materials and Methods

2.1 Reactor setup

The experimental setup is described in **Fig. 2**. The reactor (height 588 mm; inner diameter 161.5 mm) was a stainless-steel gastight tank with a water jacket for thermal regulation. The total inner volume was about 12 L, and the working volume was about 10 L. The reactor was stirred by an electric motor with an integrated magnetic coupling and three Rushton turbines (Büchi AG, Switzerland). A temperature-controlled thermostat (Labelians, France) maintained the temperature inside the reactor at 55.0 ± 0.1°C by circulating hot water in the water jacket.

The pressure in the reactor was regulated at 4.000 ± 0.001 bar with a pressure controller (Brooks Instrument, USA). The outlet gas was then analyzed by a Fusion micro gas chromatography (Inficon, Switzerland) and a drum gas meter (Ritter, Germany) measured the outlet flow rate.

CO (>99%) and CO_2 (>99.7%) were supplied with gas bottles (Air Liquide, France) whereas H_2 (>99.9999%) was obtained using a H_2 generator (Claind srl, Italy). All gases were supplied continuously, and flow rates were regulated for each gas using mass flow controllers (Brooks Instrument, USA).

The reactor was depressurized three times a week to perform liquid sampling and injections of nutrient solution, with nitrogen source. The liquid level was computed from the pressure difference between the top and the bottom of the tank, which was measured by a pressure transmitter (Keller, Switzerland).

$$k_l a_i = k_l a_{O_2} \left(\frac{D_i}{D_{O_2}} \right)^{0.5} \quad (5)$$

Mass transfer coefficients (k_La) were characterized for oxygen with the reoxygenation method by measuring dissolved oxygen concentration in clean water as described by He et al. (2003), using a EasySense O_2 21 probe (Mettler Toledo, Switzerland). The coefficients corresponding to the operational parameters (55°C – 1000 rpm – 7.5 NL/h – 4 bars) in clean water were estimated to be 27.8 ± 1.4 h^{-1} for O_2. Using the diffusivities ratio D_i/D_{O_2} according to Eq. 5, the mass transfer coefficients were then computed to be 35.2 ± 1.8 h^{-1} and 27.0 ± 1.3 h^{-1} for H_2 and CO, respectively.

2.2 Inoculation and operating conditions

The reactor was inoculated with a mesophilic anaerobic sludge sampled from the sludge digester of the municipal wastewater treatment plant of La Feyssine, Lyon, France. The inoculum was diluted to final concentrations of 11.8 ± 0.2 g/L for total solids (TS) and 8.0 ± 0.2 g/L for volatile solids (VS). Thermophilic conditions were chosen due to the higher methane productivity expected under those conditions as discussed previously and the reactor was heated at 55°C. The stirring rate was set at 1000 ± 1 rpm. Once the reactor was inoculated, the experiment started directly with a continuous gas feed of 7.500 ± 0.003 NL/h total flow rate with $H_2/CO/CO_2$ (molar ratio of 40/40/20 %). The total pressure was set

at 4 bar to apply a high CO partial pressure (1.6 ± 0.2 bar) right from the start, in order to adapt the consortium to the target pressure as discussed above.

The reactor was at first operated continuously for 50 days (Phase 1) and then had to be stopped due to lockdown measures and laboratory closure in March 2020. The adapted consortium was stored at 4°C for 78 days and then restarted for 72 days straight (Phase 2). It was decided to restart it at atmospheric pressure to check if the biological activity was still present, and the pressure was then gradually increased up to 4 bars. The two phases of continuous operations will be referred to in this paper as Phase 1 and Phase 2.

Nutrients and liquid level were regulated by adding digestate obtained by centrifugation at 5000g of the same mesophilic sludge kept at 4°C. It was analyzed for several nutrients concentrations and presented the following compositions (concentrations in mg per liter, 5% uncertainty): 0.143 B, 0.008 Co, 0.186 Cu, 0.192 Fe, 127 K, 22.6 Mg, 0.041 Ni, 5.09 S, 0.176 Zn, 714 NH_4^+. pH was maintained above 6.0 ± 0.1 by addition of NaOH (100 mg/L) or NH_4OH (25%) depending on the nitrogen requirements, with an average addition of 2 mL/d. Ammonia nitrogen –N-NH_4^+ concentration in the reactor was regularly measured according to the method described below.

From day 9 of Phase 2, a solution of $Na_2S.9H_2O$ (30 g/L) was supplied to the reactor. It was first added manually 3 times a week using a 20 mL syringe. Then from day 51, it was injected semi continuously using a dosing pump (GrundFos, Denmark). The amount added was between 5 and 10 mL/d.

2.3 Analytical Methods

Online measures included pH, temperature, pressure, inlet and outlet flows, and gas composition. The pH inside the reactor was acquired using EasySense 31 probe (Mettler Toledo, Switzerland) and temperature using a thermocouple sensor (TC Ltd, France). The composition of the outlet gas was analyzed every 15 minutes with a Fusion micro gas chromatography (Inficon, Switzerland). H_2, CO, N_2, O_2, and CH_4 were measured with a molecular sieve column and CO_2, H_2O, and H_2S with a RT-Q-Bond column. A calibration gas bottle (Air Liquide, France) was used to regularly calibrate the gas analyzer, with the following composition: 5% H_2; 5% CO; 500ppm H_2S, 60% CO_2 and CH_4 balance.

Liquid analyses included Volatile Fatty Acid (VFA), NH_4^+, trace elements, TS and VS, and water-soluble chemical oxygen demand (COD). All analyses excepting TS and VS were performed after centrifugation and filtration at 0.45 µm.

VFA were measured by ion chromatography (Shimadzu Corporation, Japan) equipped with a AS11-HC-4 µm, 2*250mm (Thermo Fisher, USA), using H_2 as carrier gas and a flame ionization detector. Water-soluble COD was measured with a LT200 mineralizer and a DR1900 HACH spectrometer. N-NH_3 were analyzed with Hack LCK303 tubes and DR1900 HACH spectrometer. Trace elements concentrations were measured by ICP-OES Ultima 2 (HORIBA Jobin Yvon, Japan) according to the NF EN ISO 11885 (1998) AFNOR NF T 90-136 Method.

The TS concentration was determined through 105°C drying for 24h and VS concentration after heating the sample at 550°C during 2h, following the ASTM standard methods recommendations.

2.4 Mass Balance Calculation Method

Mass balances calculations were done during steady-state operation phases with constant gas composition. A particular attention was paid to H_2 and CO. In the calculation, we assumed a simplified metabolic route, with CO being converted to H_2 and H_2 to CH_4. This simplification was chosen because the amount of other intermediate products was very small (See 3.1). It should be noted that due to reactions stoichiometry, the path through which secondary products are produced does not change the mass balance results. Acetate and cell production were neglected, as we computed that they represented less than 1% of the total products of reaction.

Mass balance calculations were done on specific time ranges Δt. Volatile suspended solids variations during Δt are referred to as Δm_{VSS} (g_{VSS}).

When computing H_2 conversion rates, H_2 produced from CO was taken into account in addition to injected H_2. This means that we assumed that all the CO consumed was converted into H_2 through the water gas shift reaction. This methodology allows to express the effective capability of microorganisms to convert H_2 to CH_4.

In order to study reactions kinetics, the following values were considered. $\dot{n}_i$, the molar flux of component *i* (mmol/h), is computed with the measured gas compositions and the measured total outlet flow rate.

- Production rates $[\frac{mmol}{h}]$:

$$R_{CO} = \dot{n}_{CO,\,in} - \dot{n}_{CO,\,out} \quad (6.a)$$

$$R_{H2} = [\text{Consumed injected } H_2] + [\text{Consumed } H_2 \text{ produced from CO}]$$

$$R_{H2} = [\dot{n}_{H2,\,in} - \dot{n}_{H2,\,out}] + [\dot{n}_{CO,\,in} - \dot{n}_{CO,\,out}] \quad (6.b)$$

$$R_{CH4} = \dot{n}_{CH4,\,out} \quad (6.c)$$

Production rates r_i (mmol/L_R/h) were then computed by dividing these rates by the reactor volume, and similarly specific production rates $r_{x,i}$ (mmol/g_{VSS}/h) by dividing them by Δm_{VSS}.

- Global biomass yield:

$$Y_X = \frac{Growth\ rate}{Converted\ energy} = \frac{\Delta m_{VSS}/\Delta t}{\dot{n}_{CO,\,in} - \dot{n}_{CO,\,out} + \dot{n}_{H_2,\,in} - \dot{n}_{H_2,\,out}} \left[\frac{g_{VSS}}{mol_{substrate}}\right] \quad (7)$$

Mass transfer rate is highly influenced by the gas partial pressure (Eq. 4). However, as the gas is converted throughout the reactor, its partial pressure varies and cannot be assumed equal to the applied partial pressure. For instance, when stable methanogenesis occurred, CO partial pressure was equal to 1.6 ± 0.2 bar at the inlet of the reactor, and to 0.1 ± 0.2 bar at the outlet. Hence, the logarithmic mean of the partial pressure between the entrance (P_i^{in}) and the exit (P_i^{out}) of the reactor was used to estimate the average partial pressure experienced by the microorganisms (Doran, 2013):

$$P_i^{log} = \frac{P_i^{in} - P_i^{out}}{\ln\left(P_i^{in}\right) - \ln\left(P_i^{out}\right)} [bar] \quad (8)$$

3 Results and Discussion

3.1 Water gas shift as the main intermediate reaction for methane production at 4 bars.

The results of Phase 1, obtained before the lockdown, are shown in Fig. 3. Phase 1 began at 4 bars with an early start of biological activity, starting with a decrease in CO outlet flow rate correlated with an increase in H_2 and CO_2 flow rates, indicating CO conversion into H_2 (days 1 – 5). It is more likely that CO is converted through the water-gas shift reaction (ΔG=-20 kJ/mol), which has been observed by other authors in thermophilic conditions (Grimalt-Alemany et al., 2019; Guiot et al., 2011; Sipma et al., 2003). It was then followed by a decrease in H_2 and CO_2 flow rates and an increase in CH_4 flow rate, suggesting hydrogenotrophic methanogenesis (days 5 – 20). Then we observed conversion of both H_2

and CO for a short period of time and CH_4 and CO_2 production (days 24 – 26). However, the reactor was unstable probably due to nutrients deficiency, and the results of Phase 1 were not straightforward. Indeed, no $Na_2S.9H_2O$ was added during Phase 1, and it has been suggested that it is a necessary nutrient for methanogenesis (Strübing et al., 2017).

Phase 2 started after an interruption of 78 days due to the sanitary lockdown. The biological activity was restored within the first days after restart at atmospheric pressure as described previously. At day 5 and under 1 bar, the conversion efficiency of CO and H_2 reached 87.8 ± 1.2 % and 91.0 ± 0.9 %, respectively. This result showed the high resilience of the mixed consortium, even after a long storage period at low temperature [Results not shown]. With an appropriate supply of nutrients (trace elements, sulfur, and ammonium sources) the reactor recovered a stable methane production with a full conversion of all gaseous substrates around day 10 of Phase 2. The reactor was then pressurized at 4 bars at day 17 and methane production remained stable.

Fig. 4 shows the evolution of flow rates during stable methane production periods in Phase 2 (days 30 -73). During this phase, the reactor reached stable conversion efficiencies of 99.0 ± 0.4 % and 97.6 ± 1.0 % for H_2 and CO, respectively.

The supply of sulfur was stopped on day 40 in order to stop methane production and identify intermediate mechanisms. Methane production decreased after a few days, the time for sulfur stored in the reactor to be consumed. We observed that both H_2 and CO_2 outlet flow rates increased compared to inlet flow rates, and that CO conversion still took place. This indicates that the water-gas shift reaction still occurred during this period. We had observed the same phenomenon during Phase 1. This means that H_2/CO_2 are the main products of CO conversion under these conditions. This result is consistent with previous

291 studies, showing that in thermophilic conditions, CO would be mainly converted via H_2/CO_2
292 whereas in mesophilic conditions the main intermediate seemed to be acetate (Grimalt-
293 Alemany et al., 2019).

294 *3.2 Acetate production during water gas shift phases*

295 As we can see in **Fig. 4**, the water gas-shift phase (days 44 – 57) is correlated with pH
296 decrease (from 6 – 6.5 when methanogenesis was occurring to 5.6 during the water-gas
297 shift phase). This could be due either to the higher dissolved CO_2 concentration that
298 increased as more CO_2 is produced from water-gas shift, or to the increased acetate
299 concentration.

300 Indeed, during the water-gas shift phase, we also observed an increase in acetate
301 concentration in the reactor, from around 2 g/L (day 40) up to 6 g/L during water-gas shift
302 (day 53). The same phenomenon was observed during Phase 1, with concentrations going
303 from about 3.5 g/L during methanogenesis up to about 8.5 g/L during water-gas shift (Fig.
304 3.). However, the molar balance revealed that the amount of acetate accumulated during
305 this phase represented only 0.75% of the COD consumed from CO conversion. This could
306 suggest that the acetate production is only a secondary metabolic route happening at the
307 same time as the water-gas shift reaction.

308 However, it is unclear in our case from which mechanism acetate is produced, as it can be
309 obtained either from CO (carboxydotrophic acetogenesis) or from H_2/CO_2
310 (homoacetogenesis) (**Fig. 1**). Indeed, acetate production was also observed in H_2/CO_2
311 biomethanation processes by other authors: high H_2 concentrations can lead to increased
312 acetate concentration via homoacetogenesis, in thermophilic (Kougias et al., 2017; Strübing
313 et al., 2017) and in mesophilic conditions (Agneessens et al., 2018). For instance, Liu et al.

(2016) reported that at a H_2 partial pressure of 0.96 bar, 40% of hydrogen was consumed by homoacetogens in mesophilic conditions. Nevertheless, even if acetate production from H_2 has been observed both in thermophilic and mesophilic conditions, kinetic parameters suggest that mesophilic conditions would be more favorable to homoacetogens (Rafrafi et al., 2020).

However, in the case of mixed culture syngas-biomethanation, different microorganisms could be involved. Acetate could thus be produced from various metabolic routes. Moreover, thermophilic hydrogenotrophic carboxydotrophs such as *Carboxydothermus hydrogenoformans* can shift their metabolism from hydrogenogenic to acetogenic (Henstra and Stams, 2011). Taking this into account, Grimalt-Alemany et al. (2020) when modelling syngas biomethanation, hypothesized that this shift takes place when CO conversion to H_2/CO_2 is thermodynamically limited, which occurs at high H_2 partial pressure.

In the case of thermophilic syngas-biomethanation, some elements lead to favor the hypothesis of acetate production via carboxydotrophic route rather than by homoacetogenesis. Indeed, Grimalt-Alemany et al. (2019) used activity tests with either CO, H_2/CO_2 and acetate as sole substrates and bromoethane sulfonate (BES) as inhibitory agent. They concluded that in their enrichment experiment no homoacetogenesis would occur in thermophilic conditions, whereas it would occur in mesophilic conditions. This could be in accordance with the better substrate affinity and higher maximum specific growth rate of hydrogenotrophic methanogens over homoacetogens in thermophilic conditions (Rafrafi et al., 2020), indicating higher competitivity. In contrast, in mesophilic conditions, the maximum growth rates of both groups are in the same range and homoacetogens seem to be able to outcompete hydrogenotrophic methanogens.

More experiments are required to determine if the acetate production observed in our study correlated with higher H_2 partial pressure comes from homoacetogenesis as usually observed in H_2/CO_2-biomethanation, or if it comes from a shift in CO conversion metabolism as observed in other syngas-biomethanation experiments (Diender et al., 2018; Grimalt-Alemany et al., 2019).

It should also be noted that acetate concentrations decreased after methanation restart (**Fig. 4**) around day 60, indicating acetotrophic activity. This is not in accordance with other findings that observed no acetotrophic activity in thermophilic conditions for syngas-biomethanation (Asimakopoulos et al., 2020; Grimalt-Alemany et al., 2019). However, Westman et al. (2016) when studying syngas-biomethanation with co-substrate addition containing acetate, observed an acetate conversion, indicating the presence of acetotrophic activity in thermophilic conditions. Thus, presence or not of acetotrophic activity in regard to thermophilic syngas-biomethanation requires further research.

3.3 Kinetics and productivity of syngas-biomethanation

From our results, we selected 6 periods of stable gas production to perform mass balances and to assess the conversion kinetics (they are listed **Table 1**). These periods were selected because they were associated to three different observed phenomena: methane production with conversion of all gaseous substrates (period I, III and VI), CO conversion to H_2/CO_2 with limited methane production (period IV and V, also called “water gas shift periods”), and methane production from H_2/CO_2 with limited CO conversion (period II). The fact that either CO conversion or methane production were limited during certain periods was attributed to CO inhibition (See 3.4) and nutrients deficiency (See 3.1), respectively.

The results from mass balance calculations are listed in **Table 2** . As not all gaseous substrates are converted, we hypothesized that the reactor was limited by gas-liquid mass transfer. Optimizing the mass transfer was not the purpose of this study. However, it could be improved by adding baffles to the tank (Cabaret et al., 2008). Regarding biomethanation, different reactor configurations have been studied to improve the gas-liquid mass transfer (Asimakopoulos et al., 2018), and hollow fiber membrane bioreactors appear to be the most efficient (Orgill et al., 2013; Yasin et al., 2019).

During the three methanation periods (I, III, VI), good conversion efficiencies have been observed as high as 97.6 ± 1.7 % and 98.6 ± 0.4 % for CO and H_2, respectively. H_2 conversion efficiency was always slightly higher than CO conversion efficiency, which could be explained by higher mass transfer coefficients for H_2 (35.2 ± 1.8 h^{-1}) than for CO (27.0 ± 1.3 h^{-1}).

The CO volumetric conversion rates appeared to be similar around 13 mmol/(L_R.h) during all three methanation periods. However, the CO specific rates decreased from 1.72 ± 0.11 to 1.20 ± 0.02 mmol/(g_{VSS}.h) with time. This could be explained by the growth of non carboxydotrophs microorganisms, such as methanogens for instance, leading to the overall increase of VSS and to the decrease of CO specific rate.

Furthermore, methane volumetric productivity increased over time, from 5.49 ± 3.51 during Period I to 6.80 ± 0.50 mmol/(L_R.h) during Period VI. This is probably because the VSS concentration in the reactor had increased from 7.9 ± 0.2 to 10.9 ± 0.2 gVSS/L. Indeed, the specific methane production activity was rather constant around 0.7 mmol/(g_{VSS}.h) over the three methanation periods. Those elements could also suggest a growth of

methanogenic populations, leading to an overall increase of the VSS concentration and of the methane volumetric productivity.

The global biomass yields over the three methanation periods was 0.20 g_{VSS}/mol substrate in average. This is relatively low compared to the batch experiment conducted by Grimalt-Alemany et al. (2019), where they obtained 0.66 g_{VSS}/mol substrate.

During period II, limited CO conversion (10.9 ± 8.0%) took place but methanogenesis from H_2 occurred. We can see that specific rates for H_2 conversion and CH_4 production are lower (2.25 ± 0.65 and 0.50 ± 0.07 mmol/(g_{VSS}.h), respectively) than those obtained during the methanation periods(I, III, VI) where H_2 and CH_4 specific rates were around 2.43-3.19 and 0.63-0.88 mmol/(g_{VSS}.h) respectively. This makes sense, as during period II carboxydotrophs appeared to be inhibited (See 3.4). Therefore, a portion of the overall biomass is unactive, which decreases the specific activity. Volumetric rates are also almost twice lower during Period II compared to the three methanation periods (H_2 and CH_4 volumetric rates around 13.65 ± 3.27 and 3.03 ± 0.26 mmol/(L_R.h), respectively compared to 24.58-26.07 and 5.49-6.80 for the methanation periods). This is makes sense as CO conversion to H_2 is limited.

Regarding water-gas shift periods, it can be observed that CO conversion efficiency is lower in periods IV and V when only CO conversion occurs, compared to the periods where both CO and H_2 are converted (around 91-93% versus 97-98%). However, CO mass transfer rates should be higher as less CO is converted, leading to higher CO partial pressure in the headspace. This result seems to indicate rather a thermodynamic limitation than a mass transfer issue: as H_2 is not converted, it accumulates and might limit CO conversion to H_2. Thermodynamic limitations of CO conversion to H_2 when H_2 accumulates in the headspace have already been suggested by other studies (Grimalt-Alemany et al., 2020).

An overview of some literature data of syngas-biomethanation in continuous reactors is presented in **Table 3**. When needed, the methane production rates have been converted to different units to be able to compare the results. Most of the time, the selected data correspond to the highest conversion efficiencies of the cited reference and not the highest methane productivity. It should be noted that in the biomethanation process, the performance of a given system is generally a compromise between a high methane productivity and good conversion efficiencies (Asimakopoulos et al., 2020).

To date, syngas-biomethanation research is rather new and there are very few studies with continuous processes. Moreover, the operational parameters in the existing research are highly different: reactor configuration, syngas composition, inlet syngas flow rate or microbial consortium. All these parameters have an influence on methane productivity and conversion efficiencies, hence making difficult to compare the results. Still, this literature review in Table 3 gives a comprehensive view of the current state of the art. Some trends can be noticed: for instance, higher H_2 proportion in the syngas gives higher methane production rates. This is consistent with the stoichiometry of reactions 1 and 2, which indicates that increasing H_2 proportion will increase CH_4 proportion of the produced gas within the limit of the stoichiometry and if H_2 is limiting. Moreover, this theoretical assertion has been supported by the experimental results of Li et al. (2019).

The results of the current study are promising, with methane productivity of 6.80 ± 0.50 mmolCH_4/L/h paired with good conversion efficiencies of 96.6 ± 0.3% and 98.1 ± 0.2% for CO and H_2, respectively. Steady state operation was achieved within a few days after start-up (with a mesophilic non-adapted inoculum) and restart (after the COVID sanitary lockdown and inoculum storage at 4°C), which shows the good versatility of the process.

The production rate 6.80 ± 0.50 mmolCH_4/L/h is rather high compared to results published so far. For example, Asimakopoulos et al. (2020) measured 3.80 mmolCH_4/L_R/h at similar conversion efficiencies and similar inlet flow rates in relation to reactor size (0.75 NL_{syngas}/L_R/h for this study and about 0.67 L_{syngas}/L_R/h for theirs). The difference in productivity could be explained by the slightly lower syngas flow rate, and perhaps by the difference in concentration and composition between the two consortia. In a more recent study, by increasing the inlet flow rate up to 3 L_{syngas}/L_R/h and improving the mass transfer, Asimakopoulos et al.(2021) reached 17.6 mmolCH_4/L_R/h.

By working at 4 bars, our reactor reached good conversion efficiencies and good productivity in regard to literature. Hence, working at high pressure seems a promising approach to reach high conversion efficiencies with satisfying methane productivity. However, this relies on the condition that working at higher pressure and therefore at higher CO partial pressure will not lead to CO inhibition.

3.4 CO inhibition of carboxydotrophs

The microbial inhibition by a given compound is generally due to the concentration experienced by the microorganisms. In the case of CO, the dissolved concentration results from gas to liquid mass transfer and from CO uptake by the microorganisms. In our case, as gases are converted, Pco varies in the reactor from the bottom where the gas in injected (Pco = 1.6 bar) to the top where it is vented out. Taking this into account, the logarithmic mean of the CO partial pressure in the reactor according to Eq. 8 was used to be able to study the response of the consortium to CO.

In our experiments, the mass transfer coefficient in the reactor should not vary for constant operating parameters (total gas flow rate). However, the CO partial pressure in the

450 headspace can vary during transient states as the gas composition varies with the start-up
451 of biological reactions. A transient state is represented in **Fig. 5**, with the restart of the
452 reactor after a maintenance break during Phase 2.

453 After the restart at 4 bars, we see that the first reaction was methanogenesis from H_2 (from
454 day 22 to day 24). At the same time, CO conversion did not occur. As methanogenesis from
455 H_2 decreases the quantity of moles of gas, and with no CO conversion, the proportion of CO
456 in the headspace even increased. It was then decided to reduce the total operating
457 pressure at 1 bar on day 25. This reduction of the CO partial pressure resulted in a recovery
458 of the carboxydotrophic activity in less than 24h. Our hypothesis is that high CO partial
459 pressure could inhibit the carboxydotrophic microorganisms. From day 22 to 25, the partial
460 pressure experienced by the microorganisms P_{CO}^{log} probably increased up to the inhibitory
461 limit, before CO conversion could occur and participate in decreasing P_{CO}^{log}. The reduction
462 of the total pressure probably stopped this inhibition. This demonstrates the impact of
463 P_{CO}^{log} on CO conversion kinetics.

464 This was the first time that we observed this phenomenon from the startup of the
465 experiment. Indeed, during previous startups at 4 bar the reactor was nutrient limited
466 (sulfur) and H_2 was only partially converted to CH_4. Hence, P_{CO}^{log} remained below 1.6 bars
467 from the start, allowing for CO conversion to slowly take place, resulting in a decrease of
468 P_{CO}^{log} due to CO consumption. This raises questions regarding the startup strategies of a
469 syngas-biomethanation process with an adapted consortium. In our case, this observation
470 led to a strategy following maintenance breaks consisting of a first step at atmospheric
471 pressure until the substrates conversions were stabilized, then followed by a pressure
472 increase up to 4 bar.

Fig. 5 shows that with an adapted consortium, methanogenesis from H_2 occurred under P_{CO}^{log} up to 2 bars, with H_2 conversion efficiency up to 92%. To our knowledge no previous work has studied methanogenesis from H_2 with such high P_{CO} exposure. However, at such high P_{CO}, CO conversion did not take place.

So, it appears on **Fig. 5** that after a short adaptation, methanogenesis from H_2 started quickly at high pressure compared to CO conversion. This in accordance with the findings reported by Li et al. (2020), who also observed that methanogenesis from H_2 started before CO conversion with initial 0.25 atm CO and 0.75 atm H_2. However, the authors suggested that it was due to the lower solubility of CO compared to H_2, thus inducing lower CO conversion rates. Yet, in our case, at day 22 of Phase 2, maximum mass transfer rates are estimated to 28.1 ± 4.7 mmol/(L.h) and 36.3 ± 7.9 mmol/(L.h) for CO and H_2 respectively. Those values are rather close to each other, which probably excludes CO mass transfer limitations to explain the quicker start of methanogenesis from H_2.

However, other authors studying CO-biomethanation in thermophilic conditions observed the opposite, with methanogenesis starting only after CO was fully converted (Guiot et al., 2010; Sipma et al., 2003). This seemed to indicate that CO was inhibitory to methanogenesis and carboxydotrophic hydrogenogenic activity was useful to “clean” the headspace from CO, allowing for methanogenesis to start. Yet, CO-biomethanation results and syngas-biomethanation results should be compared with caution, as it has been observed that the two enrichments methods performed on the same initial inoculum can lead to different microbial compositions (Alves et al., 2013), and therefore perhaps to different inhibition thresholds.

So, it can be deduced that, after adaptation, the microorganisms operating methanogenesis from H_2 are more resistant to CO inhibition that carboxydotrophic hydrogenogens. More experiments should be performed to determine more accurately the inhibition limit for carboxydotrophs, as we only know for now that it is with at P_{CO} at least higher than 2 bars.

Conclusions

This study has demonstrated, for the first time, the possibility for syngas-biomethanation to be operated in continuous mode at a pressure of 4 bars. The performances obtained were very promising, with methane productivity of 6.8 mmol/L_R/h and high conversion of CO (97%) and H_2 (98%). CO inhibition of carboxydotrophs was suspected in some conditions and was investigated for the first-time regarding syngas-biomethanation. Carboxydotrophs appeared to be more sensitive to CO than methanogens and to be inhibited at CO partial pressure higher than 2 bars. Overall, this study demonstrated that syngas-biomethanation in a pressurized reactor is a promising approach to industrialization.

Acknowledgements

The authors would like to thank ENOSIS for the financial support, Richard Poncet and Hervé Périer-Camby for the original experimental setup, Nathalie Dumont and David Le Bouil for the chemical analysis. This work was performed within the framework of the EUR H2O'Lyon (ANR-17-EURE-0018) of Université de Lyon (UdL), within the program "Investissements d'Avenir" operated by the French National Research Agency (ANR).

516 **Figure Captions**

517 **Fig. 1.** Simplified representation of biological mechanisms involved in syngas
518 biomethanation by a mixed consortium (Rafrafi et al., 2020). SAO: Syntrophic Acetate
519 Oxidation.

520 **Fig. 2.** Simplified scheme of the reactor system. (1) tank, (2) stirring system, (3) pressurized
521 sulfide circuit, (4) thermostat, (5) CO gas bottle, (6) CO mass flow controller, (7) CO_2 gas
522 bottle, (8) CO_2 mass flow controller, (9) H_2 generator, (10) H_2 mass flow controller, (11)
523 liquid addition or withdraw, (12) pressure controller, (13) gas analyzer, (14) drum gas
524 counter.

525 **Fig. 3.** Outlet flow rates (A) pH, and acetate, propionate and volatile solids concentrations
526 (B) during operational days 0-50 of Phase 1. Data acquisition of outlet flow rates was
527 interrupted due to technical difficulties from day 13 to 15, 18 to 19 and 48 to 50.

528 **Fig. 4.** Outlet flow rates (A) pH, acetate, propionate and volatile solids concentrations (B)
529 during operational days 30-73 of Phase 2. Data acquisition of outlet flow rates was
530 interrupted due to technical difficulties from day 57 to 60.

531 **Fig. 5.** Effect of P_{CO}^{log} during Phase 2, after a maintenance break of the reactor at day 22.

532 **Tables and Figures**

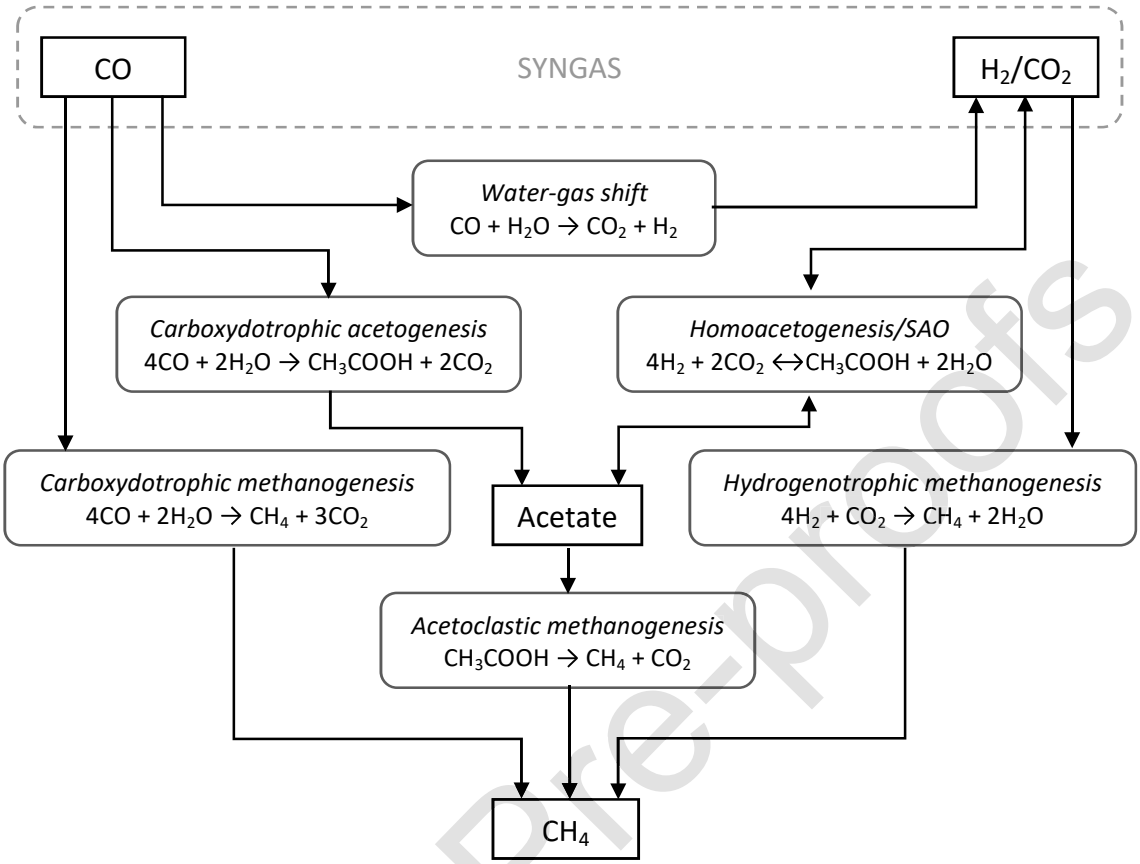

533
534 Figure 1

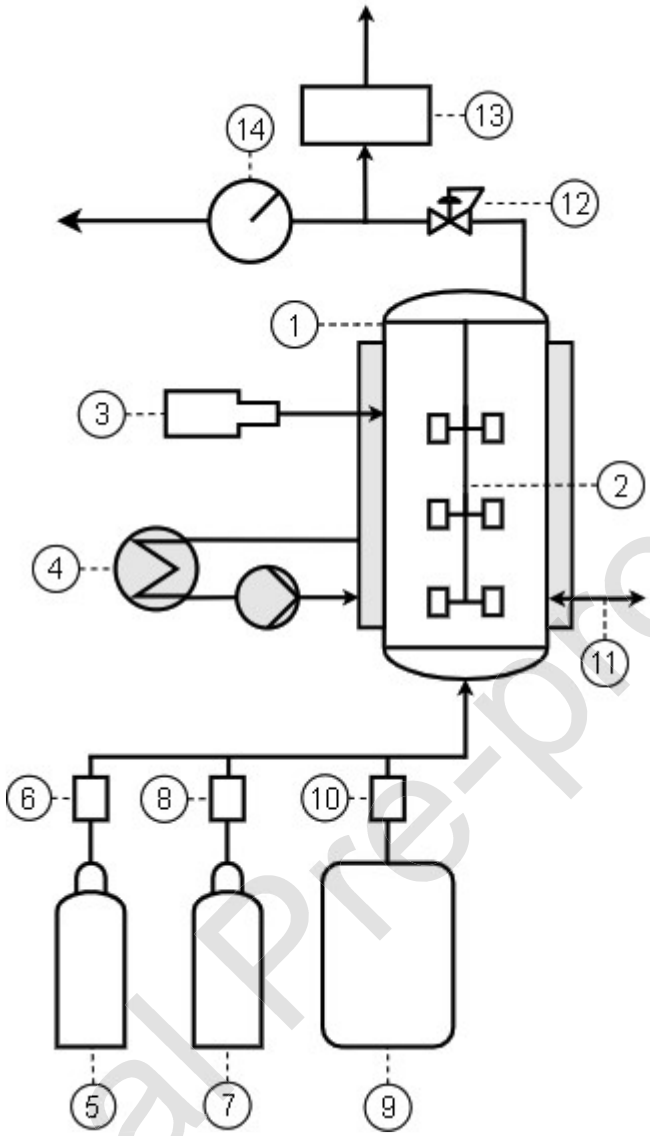

535

536 Figure 2

537

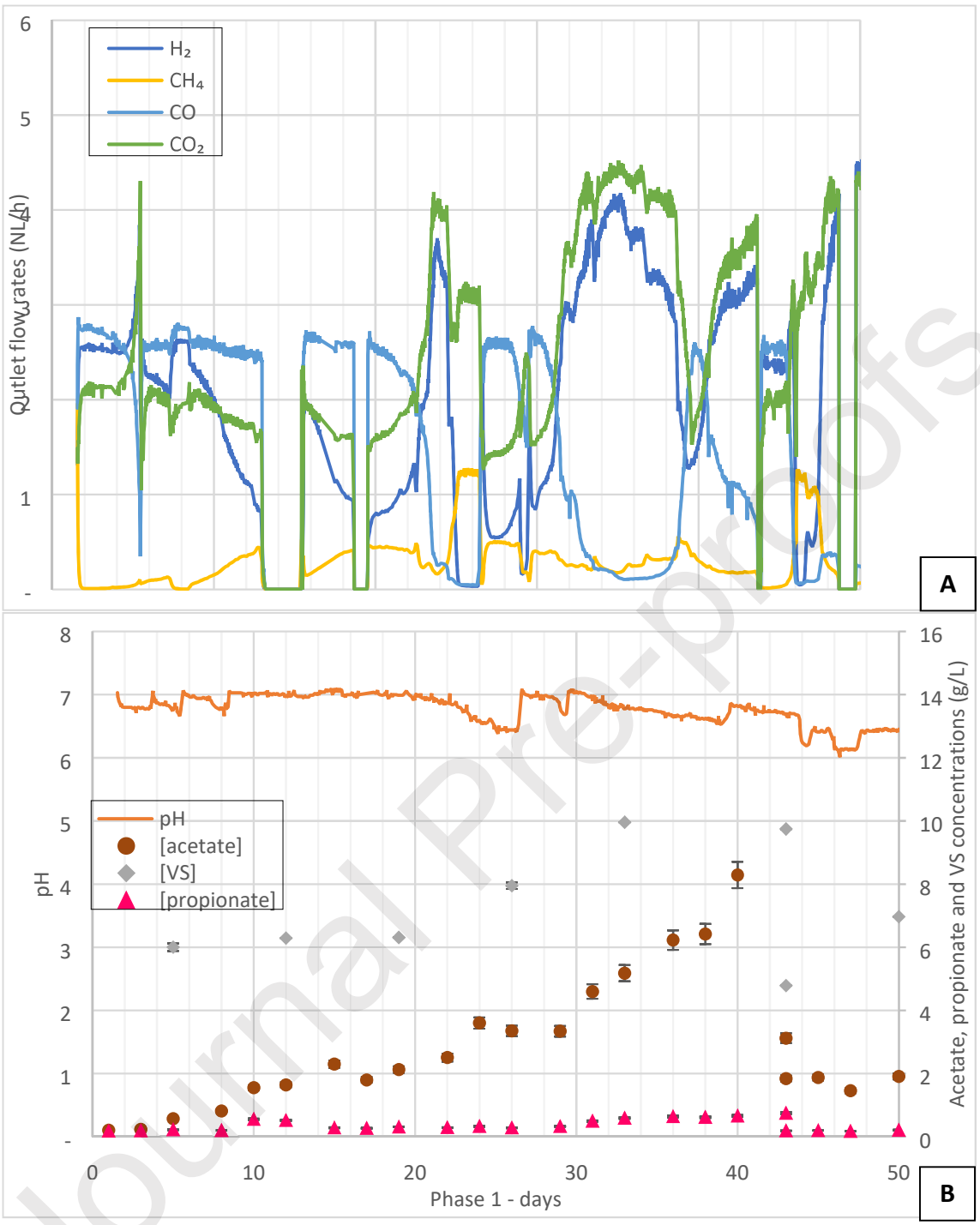

538

539 Figure 3

540

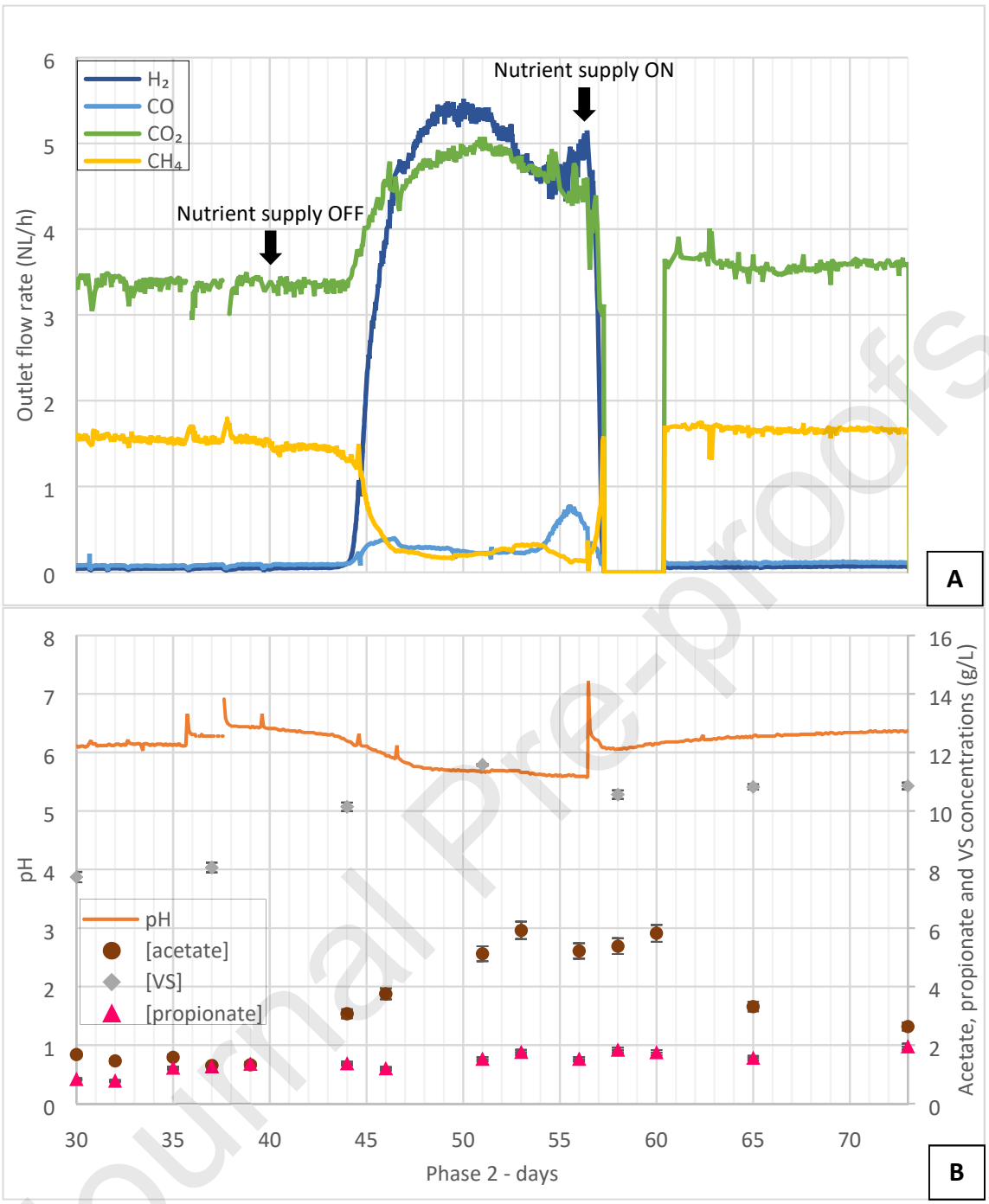

Figure 4

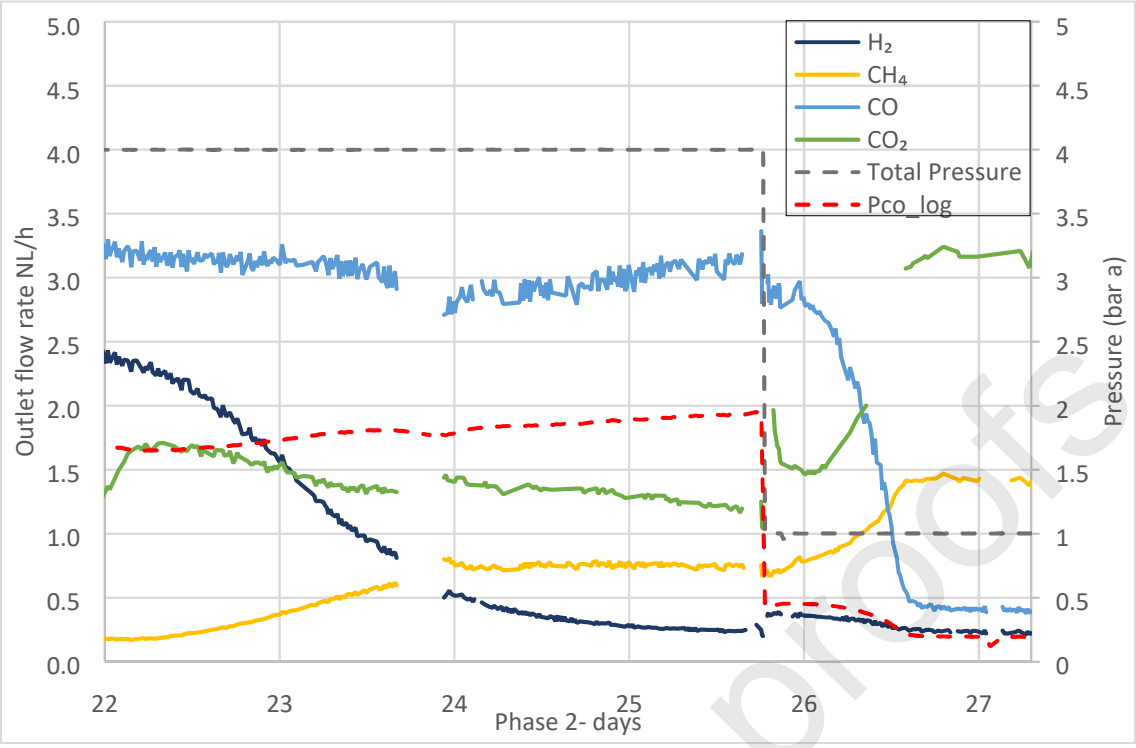

Figure 5

549

550 **Table 1 :** Selected steady-state periods for mass balance calculations.

N°	Date	reaction description
I	Phase 1 - day 24-26	Methanogenesis from H_2/CO_2 with CO conversion
II	Phase 2 – day 24-25	Methanogenesis from H_2/CO_2 – limited CO conversion
III	Phase 2– day 30-39	Methanogenesis from H_2/CO_2 with CO conversion
IV	Phase 2– day 47-49	WgS : CO conversion to H_2/CO_2 – limited methane production
V	Phase 2– day 49-53	WgS : CO conversion to H_2/CO_2 – limited methane production
VI	Phase 2– day 60-73	Methanogenesis from H_2/CO_2 with CO conversion

551 WgS: water gas shift

552

553 **Table 2 :** Mass balance and specific rates during steady-state periods.

	Water Gas Shift periods		Limited CO conversion period	Methanation periods		
	IV	V	II	I	III	VI
Conversion efficiencies (%)						
X_{CO}	91.3% ± 0.6%	92.9% ± 0.6%	10.9% ± 8.0%	97.8% ± 1.7%	97.6% ± 1.0%	96.6% ± 0.3%
X_{H_2}	-56.9% ± 7.3%	-55.2% ± 7.9%	90.8% ± 2.2%	89.2% ± 19.1%	98.6% ± 0.4%	98.1% ± 0.2%
Volumetric rates [mmol/(L_R.h)]						
r_{CO}	12.22 ± 0.21	12.43 ± 0.21	1.46 ± 2.66	12.85 ± 0.47	12.98 ± 0.26	12.94 ± 0.10
r_{H_2}	4.60 ± 2.58	5.04 ± 2.80	13.65 ± 3.27	24.58 ± 6.15	26.10 ± 0.41	26.07 ± 0.17
r_{CH_4}	0.80 ± 0.15	1.01 ± 0.24	3.03 ± 0.26	5.49 ± 3.51	6.62 ± 2.07	6.80 ± 0.50
Specific rates [mmol/(g_{VSS}.h)]						
$r_{X,\,CO}$	1.15 ± 0.04	1.11 ± 0.02	0.24 ± 0.45	1.67 ± 0.11	1.58 ± 0.12	1.20 ± 0.02
$r_{X,\,H_2}$	0.43 ± 0.25	0.45 ± 0.25	2.25 ± 0.65	3.19 ± 0.89	3.18 ± 0.23	2.43 ± 0.04
$r_{X,\,CH_4}$	0.08 ± 0.02	0.09 ± 0.02	0.50 ± 0.07	0.71 ± 0.48	0.88 ± 0.28	0.63 ± 0.05

Table 3 : Overview of existing continuous reactors in literature. Most production rates have been converted to unify the units. V: working volume, T: temperature, X_{CO} and X_{H_2}: conversion efficiencies of CO and H_2 respectively, r_{CH_4} : volumetric methane production rate, r_{X,CH_4}: specific methane production rate, CSTR: Continuous Stirred Tank Reactor, NM: not mentioned.

	Reactor type	Pressure	Microbial inoculum	V (L)	T(°C)	Syngas composition	X_{CO} (%)	X_{H_2} (%)	r_{CH_4} [mmol/(L_R.h)]
Current work	Pressurized agitated column	4 bars (a)	Mixed Microbial Consortia	10	55	40% H_2, 20% CO_2, 40% CO	97	98	6.8
Asimakopoulos et al. (2020)	Trickle bed reactor	NM	Mixed Microbial Consortia	0.18	60	45% H_2, 25% CO_2, 20% CO, 10% N_2	73	89	8.49
Asimakopoulos et al. (2020)	Trickle bed reactor	NM	Mixed Microbial Consortia	0.18	60	45% H_2, 25% CO_2, 20% CO, 10% N_2	96	98	3.80
Asimakopoulos et al. (2021)	Trickle bed reactor	1 bar	Mixed Microbial Consortia	5	60	45% H_2, 25% CO_2, 20% CO, 10% N_2	98	100	10.6
Asimakopoulos et al. (2021)	Trickle bed reactor	1 bar	Mixed Microbial Consorita	5	60	45% H_2, 25% CO_2, 20% CO, 10% N_2	76.3	96.7	17.6
Chandolias et al. (2019)	Floating membrane reactor	NM	Mixed Microbial Consortia	1.7	55	20% H_2, 55% CO, 10% CO_2, 15% N_2, acetate	16	19	1.43
Diender et al., (2018)	CSTR	1 bar	Coculture	0.75	65	66.6% H_2, 33.3% CO	93	97	7.44*
Westman et al. (2016)	Reverse membrane bioreactor	NM	Mixed Microbial Consortia	0.6	55	20% H_2, 55% CO, 10% CO_2, 15% N_2	100**	100**	0.2*
Westman et al. (2016)	Free cells bioreactor	NM	Mixed Microbial Consortia	0.6	55	20% H_2, 55% CO, 10% CO_2, 15% N_2	100**	100**	0.2
Sun et al. (2020)	In situ biomethanation	NM	Mixed Microbial Consortia	37.5	37	50% H_2, 50% CO	94	100	0.46***
Kimmel et al. (1991)	Trickle bed reactor	1 bar	Triculture	1.05	37	14.82% Ar, 9.67% CO_2, 55.62% CO, 19.68% H_2	70	NM	3.00
Kimmel et al. (1991)	Trickle bed reactor	1 bar	Triculture	26.05	37	14.74% Ar, 9.72% CO_2, 54.42% CO, 21.11% H_2	38	NM	0.12

*This result is higher than the maximum theoretical stoichiometric value.

**Full conversion has probably been achieved because of gas recirculation.

***Methane produced from syngas only was considered, not from added glucose

References

Agneessens, L.M., Ottosen, L.D.M., Andersen, M., Berg Olesen, C., Feilberg, A., Kofoed, M.V.W., 2018. Parameters affecting acetate concentrations during in-situ biological hydrogen methanation. Bioresour. Technol. 258, 33–40. https://doi.org/10.1016/j.biortech.2018.02.102

Alves, J.I., Stams, A.J.M., Plugge, C.M., Madalena Alves, M., Sousa, D.Z., 2013. Enrichment of anaerobic syngas-converting bacteria from thermophilic bioreactor sludge. FEMS Microbiol. Ecol. 86, 590–597. https://doi.org/10.1111/1574-6941.12185

Alves, J.I.F., 2013. Microbiology of thermophilic anaerobic syngas conversion (PhD Thesis).

Arantes, A.L., Alves, J.I., Stams, A.J., Alves, M.M., Sousa, D.Z., 2018. Enrichment of syngas-converting communities from a multi-orifice baffled bioreactor. Microb. Biotechnol. 11, 639–646.

Arena, U., 2012. Process and technological aspects of municipal solid waste gasification. A review. Waste Manag. 32, 625–639. https://doi.org/10.1016/j.wasman.2011.09.025

Asimakopoulos, K., Gavala, H.N., Skiadas, I.V., 2018. Reactor systems for syngas fermentation processes: A review. Chem. Eng. J. 348, 732–744. https://doi.org/10.1016/j.cej.2018.05.003

Asimakopoulos, K., Kaufmann-Elfang, M., Lundholm-Høffner, C., Rasmussen, N.B.K., Grimalt-Alemany, A., Gavala, H.N., Skiadas, I.V., 2021. Scale up study of a thermophilic trickle bed reactor performing syngas biomethanation. Appl. Energy 290, 116771. https://doi.org/10.1016/j.apenergy.2021.116771

Asimakopoulos, K., Łężykb, M., Grimalt-Alemany, A., Melas, A., Wen, Z., Gavala, H.N., Skiadas, I.V., 2020. Temperature effects on syngas biomethanation performed in a trickle bed reactor. Chem. Eng. J. 13.

Beck, J.V., 1971. Chapter 8 - Enrichment culture and isolation techniques particularly for anaerobic bacteria, in: Methods in Enzymology. Elsevier, pp. 57–64. https://doi.org/10.1016/0076-6879(71)22010-3

Bu, F., Dong, N., Kumar Khanal, S., Xie, L., Zhou, Q., 2018. Effects of CO on hydrogenotrophic methanogenesis under thermophilic and extreme-thermophilic conditions: Microbial community and biomethanation pathways. Bioresour. Technol. 266, 364–373. https://doi.org/10.1016/j.biortech.2018.03.092

Cabaret, F., Fradette, L., Tanguy, P.A., 2008. Gas–liquid mass transfer in unbaffled dual-impeller mixers. Chem. Eng. Sci. 63, 1636–1647. https://doi.org/10.1016/j.ces.2007.11.028

Chandolias, K., Pekgenc, E., Taherzadeh, M., 2019. Floating Membrane Bioreactors with High Gas Hold-Up for Syngas-to-Biomethane Conversion. Energies 12, 1046. https://doi.org/10.3390/en12061046

Diender, M., Uhl, P.S., Bitter, J.H., Stams, A.J.M., Sousa, D.Z., 2018. High Rate Biomethanation of Carbon Monoxide-Rich Gases via a Thermophilic Synthetic Coculture. ACS Sustain. Chem. Eng. 6, 2169–2176. https://doi.org/10.1021/acssuschemeng.7b03601

Doran, P.M., 2013. Chapter 10 - Mass Transfer, in: Bioprocess Engineering Principles (Second Edition). Elsevier, pp. 379–444. https://doi.org/10.1016/B978-0-12-220851-5.00010-1

Grimalt-Alemany, A., Asimakopoulos, K., Skiadas, I.V., Gavala, H.N., 2020. Modeling of syngas biomethanation and catabolic route control in mesophilic and thermophilic

mixed microbial consortia. Appl. Energy 262, 114502. https://doi.org/10.1016/j.apenergy.2020.114502

Grimalt-Alemany, A., Łężyk, M., Kennes-Veiga, D.M., Skiadas, I.V., Gavala, H.N., 2019. Enrichment of Mesophilic and Thermophilic Mixed Microbial Consortia for Syngas Biomethanation: The Role of Kinetic and Thermodynamic Competition. Waste Biomass Valorization. https://doi.org/10.1007/s12649-019-00595-z

Grimalt-Alemany, A., Skiadas, I.V., Gavala, H.N., 2018. Syngas biomethanation: state-of-the-art review and perspectives. Biofuels Bioprod. Biorefining 12, 139–158.

Guiot, S.R., Cimpoia, R., Carayon, G., 2011. Potential of Wastewater-Treating Anaerobic Granules for Biomethanation of Synthesis Gas. Environ. Sci. Technol. 45, 2006–2012. https://doi.org/10.1021/es102728m

Guiot, S.R., Cimpoia, R., Carayon, G., 2010. Biomethanation of synthesis gas using anaerobic granules within a closed loop gas lift reactor.

He, Z., Petiraksakul, A., Meesapya, W., 2003. Oxygen-Transfer Measurement in Clean Water 13, 6.

Henstra, A.M., Stams, A.J.M., 2011. Deep Conversion of Carbon Monoxide to Hydrogen and Formation of Acetate by the Anaerobic Thermophile *Carboxydothermus hydrogenoformans*. Int. J. Microbiol. 2011, 1–4. https://doi.org/10.1155/2011/641582

Kimmel, D.E., Klasson, K.T., Clausen, E.C., Gaddy, J.L., 1991. Performance of trickle-bed bioreactors for converting synthesis gas to methane. Appl. Biochem. Biotechnol. 28–29, 457–469. https://doi.org/10.1007/BF02922625

Klasson, K.T., Ackerson, M.D., Clausen, E.C., Gaddy, J.L., 1991. Bioreactors for synthesis gas fermentations. Resour. Conserv. Recycl. 5, 145–165. https://doi.org/10.1016/0921-3449(91)90022-G

Kougias, P.G., Treu, L., Benavente, D.P., Boe, K., Campanaro, S., Angelidaki, I., 2017. Ex-situ biogas upgrading and enhancement in different reactor systems. Bioresour. Technol. 225, 429–437. https://doi.org/10.1016/j.biortech.2016.11.124

Li, C., Zhu, X., Angelidaki, I., 2020. Carbon monoxide conversion and syngas biomethanation mediated by different microbial consortia. Bioresour. Technol. 314, 123739. https://doi.org/10.1016/j.biortech.2020.123739

Li, Y., Wang, Z., He, Z., Luo, S., Su, D., Jiang, H., Zhou, H., Xu, Q., 2019. Effects of temperature, hydrogen/carbon monoxide ratio and trace element addition on methane production performance from syngas biomethanation. Bioresour. Technol. 122296. https://doi.org/10.1016/j.biortech.2019.122296

Liu, R., Hao, X., Wei, J., 2016. Function of homoacetogenesis on the heterotrophic methane production with exogenous H 2 /CO 2 involved. Chem. Eng. J. 284, 1196–1203. https://doi.org/10.1016/j.cej.2015.09.081

Luo, G., Wang, W., Angelidaki, I., 2013. Anaerobic Digestion for Simultaneous Sewage Sludge Treatment and CO Biomethanation: Process Performance and Microbial Ecology. Environ. Sci. Technol. 130904143045005. https://doi.org/10.1021/es401018d

Oremland, R.S., Capone, D.G., 1988. Use of “Specific” Inhibitors in Biogeochemistry and Microbial Ecology, in: Marshall, K.C. (Ed.), Advances in Microbial Ecology. Springer US, Boston, MA, pp. 285–383. https://doi.org/10.1007/978-1-4684-5409-3_8

Orgill, J.J., Atiyeh, H.K., Devarapalli, M., Phillips, J.R., Lewis, R.S., Huhnke, R.L., 2013. A comparison of mass transfer coefficients between trickle-bed, hollow fiber

membrane and stirred tank reactors. Bioresour. Technol. 133, 340–346. https://doi.org/10.1016/j.biortech.2013.01.124

Perkins, G., 2020. Production of electricity and chemicals using gasification of municipal solid wastes, in: Waste Biorefinery. Elsevier, pp. 3–39. https://doi.org/10.1016/B978-0-12-818228-4.00001-0

Rafrafi, Y., Laguillaumie, L., Dumas, C., Figueras, J., 2020. Biological Methanation of H2 and CO2 with Mixed Cultures: Current Advances, Hurdles and Challenges. Waste Biomass Valorization. https://doi.org/10.1007/s12649-020-01283-z

Sancho Navarro, S., Cimpoia, R., Bruant, G., Guiot, S.R., 2016. Biomethanation of Syngas Using Anaerobic Sludge: Shift in the Catabolic Routes with the CO Partial Pressure Increase. Front. Microbiol. 7. https://doi.org/10.3389/fmicb.2016.01188

Sipma, J., Lens, P.N.L., Stams, A.J.M., Lettinga, G., 2003. Carbon monoxide conversion by anaerobic bioreactor sludges. FEMS Microbiol. Ecol. 44, 271–277. https://doi.org/10.1016/S0168-6496(03)00033-3

Sipma, J., Meulepas, R.J.W., Parshina, S.N., Stams, A.J.M., Lettinga, G., Lens, P.N.L., 2004. Effect of carbon monoxide, hydrogen and sulfate on thermophilic (55°C) hydrogenogenic carbon monoxide conversion in two anaerobic bioreactor sludges. Appl. Microbiol. Biotechnol. 64, 421–428. https://doi.org/10.1007/s00253-003-1430-4

Strübing, D., Huber, B., Lebuhn, M., Drewes, J.E., Koch, K., 2017. High performance biological methanation in a thermophilic anaerobic trickle bed reactor. Bioresour. Technol. 245, 1176–1183. https://doi.org/10.1016/j.biortech.2017.08.088

Sun, H., Yang, Z., Zhao, Q., Kurbonova, M., Zhang, R., Liu, G., Wang, W., 2020. Modification and extension of Anaerobic Digestion Model No.1 (ADM1) for syngas biomethanation simulation: From lab-scale to pilot-scale. Chem. Eng. J. 126177. https://doi.org/10.1016/j.cej.2020.126177

Westman, S., Chandolias, K., Taherzadeh, M., 2016. Syngas Biomethanation in a Semi-Continuous Reverse Membrane Bioreactor (RMBR). Fermentation 2, 8. https://doi.org/10.3390/fermentation2020008

Yasin, M., Cha, M., Chang, I.S., Atiyeh, H.K., Munasinghe, P., Khanal, S.K., 2019. Syngas Fermentation Into Biofuels and Biochemicals, in: Biofuels: Alternative Feedstocks and Conversion Processes for the Production of Liquid and Gaseous Biofuels. Elsevier, pp. 301–327. https://doi.org/10.1016/B978-0-12-816856-1.00013-0

Youngsukkasem, S., Chandolias, K., Taherzadeh, M.J., 2015. Rapid bio-methanation of syngas in a reverse membrane bioreactor: Membrane encased microorganisms. Bioresour. Technol. 178, 334–340. https://doi.org/10.1016/j.biortech.2014.07.071

Declaration of interests

☒ The authors declare that they have no known competing financial interests or personal relationships that could have appeared to influence the work reported in this paper.

☐The authors declare the following financial interests/personal relationships which may be considered as potential competing interests:

- A continuous pressurized bioreactor has been run for syngas biomethanation.
- A high methane productivity and high CO and H2 conversions were achieved.
- CO inhibition on carboxydotrophs was a possible cause of limitation.